

See discussions, stats, and author profiles for this publication at: <https://www.researchgate.net/publication/235393845>

# Metal-Enzyme Frameworks: Role of Metal Ions in Promoting Enzyme Self-Assembly on $\alpha$ -Zirconium(IV) Phosphate Nanoplates

ARTICLE in LANGMUIR · FEBRUARY 2013

Impact Factor: 4.46 · DOI: 10.1021/la304979s · Source: PubMed

---

CITATIONS

14

---

READS

36

## 4 AUTHORS, INCLUDING:



[Ajith Pattammattel](#)

University of Connecticut

9 PUBLICATIONS 24 CITATIONS

[SEE PROFILE](#)



[Inoka K Deshapriya](#)

University of Connecticut

11 PUBLICATIONS 47 CITATIONS

[SEE PROFILE](#)



[Challa V Kumar](#)

University of Connecticut

186 PUBLICATIONS 5,745 CITATIONS

[SEE PROFILE](#)

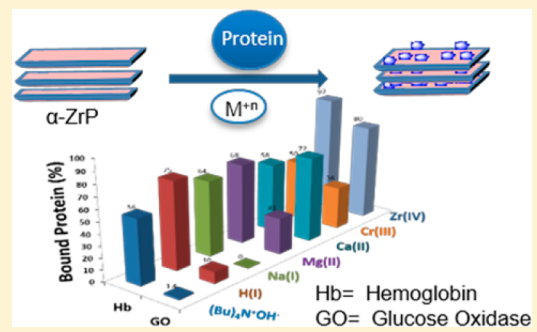
## Metal-Enzyme Frameworks: Role of Metal Ions in Promoting Enzyme Self-Assembly on $\alpha$ -Zirconium(IV) Phosphate Nanoplates

Ajith Pattammattel, Inoka K. Deshapriya, Ruma Chowdhury, and Challa V. Kumar\*

Departments of Chemistry and Molecular & Cell Biology, University of Connecticut, U-3060, Storrs, Connecticut 06269, United States

 Supporting Information

**ABSTRACT:** Previously, an ion-coupled protein binding (ICPB) model was proposed to explain the thermodynamics of protein binding to negatively charged  $\alpha$ -Zr(IV) phosphate ( $\alpha$ -ZrP). This model is tested here using glucose oxidase (GO) and met-hemoglobin (Hb) and several cations (Zr(IV), Cr(III), Au(III), Al(III), Ca(II), Mg(II), Zn(II), Ni(II), Na(I), and H(I)). The binding constant of GO with  $\alpha$ -ZrP was increased  $\sim$ 380-fold by the addition of either 1 mM Zr(IV) or 1 mM Ca(II), and affinities followed the trend  $Zr(IV) \approx Ca(II) > Cr(III) > Mg(II) \gg H(I) > Na(I)$ . Binding studies could not be conducted with Au(III), Al(III), Zn(II), Cu(II), and Ni(II), as these precipitated both proteins. Zr(IV) increased Hb binding constant to  $\alpha$ -ZrP by 43-fold, and affinity enhancements followed the trend  $Zr(IV) > H(I) > Mg(II) > Na(I) > Ca(II) > Cr(III)$ . Zeta potential studies clearly showed metal ion binding to  $\alpha$ -ZrP and affinities followed the trend,  $Zr(IV) \gg Cr(III) > Zn(II) > Ni(II) > Mg(II) > Ca(II) > Au(III) > Na(I) > H(I)$ . Electron microscopy showed highly ordered structures of protein/metal/ $\alpha$ -ZrP intercalates on micrometer length scales, and protein intercalation was also confirmed by powder X-ray diffraction. Specific activities of GO/Zr(IV)/ $\alpha$ -ZrP and Hb/Zr(IV)/ $\alpha$ -ZrP ternary complexes were  $2.0 \times 10^{-3}$  and  $6.5 \times 10^{-4} M^{-1} s^{-1}$ , respectively. While activities of all GO/cation/ $\alpha$ -ZrP samples were comparable, those of Hb/cation/ $\alpha$ -ZrP followed the trend  $Mg(II) > Na(I) > H(I) > Cr(III) > Ca(II) \approx Zr(IV)$ . Metal ions enhanced protein binding by orders of magnitude, as predicted by the ICPB model, and binding enhancements depended on charge as well as the phosphophilicity/oxophilicity of the cation.



### 1. INTRODUCTION

Protein self-assembly at liquid–solid interfaces is of current interest, and this is often achieved via chemical,<sup>1</sup> biomolecular,<sup>2</sup> thermal,<sup>3</sup> or metal-induced<sup>4–6</sup> assembly. Protein self-assembly is challenging because of the large size of proteins, multiple functional groups on their surfaces, their fragility to solvents, sensitivity to particular ions and extreme pH, and their vulnerability to degradation by proteases, which are ubiquitous. Protein assemblies are increasingly being used in biosensing,<sup>7</sup> biomaterials,<sup>8</sup> biocatalysis,<sup>9</sup> and biomedicine.<sup>10</sup> Therefore, it is critical to understand how such assemblies can be constructed by a systematic approach and establish the details of the mechanism of protein assembly, so that protein assembly can be controlled in a rational, predictable manner. Despite the widespread interest in the application of proteins bound to solid surfaces, there are no quantitative models or rational approaches to address these important issues.

The mechanism of protein binding to solid surfaces is complex, not fully understood,<sup>11</sup> but in the case of most water-soluble, charged proteins, protein binding requires charge neutralization at the protein–solid interface, and this electrostatic requirement imposes the participation of appropriately charged species (ions) in the protein binding mechanism. Although, there have been several qualitative studies on the promotion of binding of anionic biomolecules such as DNA to

negatively charged solids such as mica,<sup>12–15</sup> or other solids,<sup>16</sup> there have been no quantitative studies evaluating the role of metal ions in biomolecule binding to ionic solids.

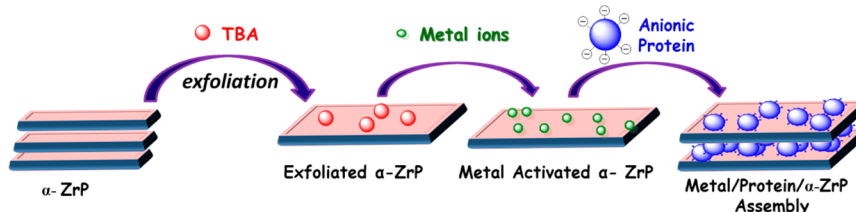
Previously, protein binding to charged solid surfaces was proposed to involve the sequestration or release of ions at/from the protein–solid interface.<sup>17,18</sup> That is, binding of negatively charged proteins to negatively charged solid would require sequestration of cations of proper charge, affinity and concentration to support protein binding.<sup>17,18</sup> The ion sequestration at the interface would neutralize the excess charge and facilitate protein assembly, and this ion-coupled protein binding (ICPB) model, where the metal ions played a critical role in protein binding, was also supported by pH and temperature dependence studies.<sup>17</sup>

Here, the ICPB model is tested explicitly, and we demonstrate metal-mediated binding of two model proteins glucose oxidase (GO) and met-hemoglobin (Hb) to anionic  $\alpha$ -zirconium(IV) phosphate ( $Zr(HPO_4)_2 \cdot H_2O$ , abbreviated as  $\alpha$ -ZrP).<sup>19,20</sup>  $\alpha$ -ZrP consists of chemically and topologically homogeneous nanosheets, with large surface area per unit mass and high charge density. The stacks of  $\alpha$ -ZrP nanosheets

Received: July 30, 2012

Revised: February 1, 2013

Published: February 1, 2013

**Scheme 1.** Cation-Induced Binding of Anionic Proteins to  $\alpha$ -ZrP Nanosheets

are exfoliated with tetrabutylammonium chloride<sup>21</sup> to bind metal ions, small molecules, metal complexes, and proteins, regardless of their size.<sup>11,22,23</sup> Protein/α-ZrP assemblies, for example, indicated better thermal stability of the intercalated proteins, and the structure as well as the biological activities of the intercalated proteins have been retained to a significant extent.<sup>16</sup> However, one issue with α-ZrP is that its affinity for negatively charged proteins is often quite low due to unfavorable charge–charge interactions with the solid.<sup>10</sup> Consistent with this evaluation, we previously noted that conversion of the anionic proteins to the corresponding cationic-derivatives, via chemical modification of the surface carboxyl groups to the corresponding amide derivatives, enhanced protein binding affinities to α-ZrP.<sup>24</sup>

According to the ICPB model, high affinity binding of anionic proteins to anionic α-ZrP requires sequestration of appropriate cations at the protein–solid interface to neutralize the excess negative charge. Therefore, we examined the binding of GO (isoelectric point, pI, of 4.0,<sup>25</sup>) and Hb (pI = 6.7) to α-ZrP nanodiscs and the role of a few metal ions, Zr(IV), Au(III), Cr(III), Mg(II), Zn(II), Ni(II), Ca(II), Na(I), and H(I) in the binding mechanism. GO is chosen for its importance as a biocatalyst, and it catalyzes the conversion of β-D-glucose to δ-gluconolactone while reducing ambient O<sub>2</sub> to H<sub>2</sub>O<sub>2</sub>.<sup>26–28</sup> Hb does not function as an enzyme in nature, but its role as a peroxidase is well-known.<sup>29</sup> Both GO and Hb are negatively charged at neutral pH,<sup>30</sup> and their binding to α-ZrP should be influenced by metal ions. The selection of the cations for the current studies depended on several factors. We chose pH 3 for these studies, since 1 mM Zr(IV) (pH 3) indicated the highest increases of protein binding to α-ZrP. Au(III), Cr(III), Al(III), Zn(II), Ni(II), and Cu(II) precipitated these two proteins even at pH 3, while many others were not soluble in water at pH 3. Systematic variation of charge, size, and chemical nature of the metal ions provided valuable insight into the role of these ions in the binding mechanism.

Zr(IV) is strongly oxophilic and coordinates readily with the carboxyl groups of aspartate and glutamate residues of proteins.<sup>31</sup> It binds to the iron-transporter protein,<sup>32</sup> β-casein,<sup>33</sup> and the phosphate groups of α-ZrP,<sup>34</sup> and thereby it could potentially function as a metal glue between the anionic proteins and the anionic α-ZrP (Scheme 1). Zr(IV)-activated phosphate/phosphonate surfaces were used to study biomolecular interactions<sup>35</sup> where the metal mediated the binding.<sup>36</sup> Tetravalent Zr(IV) was expected to have greater binding affinity when compared to trivalent or lower valent metal ions. Many trivalent metal ions could not be used for the current studies, as these tended to precipitate both proteins even at 1 mM metal concentration and pH 3. Ca(II) is known to have a higher sorption to α-ZrP over other divalent metal ions,<sup>37</sup> and Ca(II) was expected to bind to the COOH groups of anionic proteins with moderate to high affinities.<sup>38</sup> Mg(II) also coordinates to certain amino acids and phosphate groups on

proteins, even though much more weakly than Ca(II) or Zr(IV).<sup>39</sup>

Many divalent and monovalent metal ions have poor coordination abilities for monovalent ligands, but they have better affinities for polyacids and polyamines due to the chelate effect.<sup>40</sup> Generally, protein surfaces have numerous carboxyl and amino groups which are appropriate for the coordination of metal ions. Na(I) and H(I) are selected as the monovalent ions for our studies, and H(I) is required to adjust the pH to 3 to solubilize the above metal salts. Na(I) is commonly used in many buffers and served as a good control to compare with H(I). Zr(IV), Cr(III), Ca(II), Mg(II), H(I), and Na(I) provided a simple series to test the role of metal ions on protein binding to α-ZrP. It is not obvious how the charge or the coordination abilities of metal ions promote or even inhibit protein binding, and it is not clear how metal-mediation would depend on the nature of the protein. For example, metal ions can enhance binding due to neutralization of α-ZrP negative charge, or they could inhibit binding due to increased ionic strength or by competing for the phosphate groups of α-ZrP. Therefore, it is not obvious how these opposing contributions depend on the nature of metal ions, metal concentration and nature of the protein. Here, we clearly establish a method to enhance protein binding using metal ions and clearly demonstrate that the nature of the metal ion (oxophilicity and phosphophilicity) plays an important role in protein binding. The metal behavior did not depend solely on its charge, size, or coordination behavior, and could not be predicted a priori. Conceptually, both oxophilicity as well as the phosphophilicity of the metal ion determine its ability to promote protein binding. Thus, current studies are justified to evaluate these important aspects.

Our data show that metal ions play a major role in protein binding to α-ZrP, in support of ICPB mechanism. Zr(IV) turned out to be the best metal glue for both proteins, while Ca(II) promoted the binding of GO much better than that of Hb. Thus, binding enhancement depended on both the metal ion as well as the isoelectric point of the protein.

## 2. MATERIALS AND METHODS

Glucose oxidase (GO, *Aspergillus niger*, 90%) and peroxidase type 1 from horseradish (HRP; specific activity of 356 U/mg) were purchased from Calzyme Laboratories Inc. (San Luis Obispo, CA) and used without further purification. Bovine met-hemoglobin (Hb), glucose, guaiacol, ZrOCl<sub>2</sub>, and all metal chlorides were purchased from Sigma-Aldrich Co (St. Louis, MO). Carbon coated TEM grids were purchased from Ted Pella Inc.

**2.1. Synthesis of α-ZrP.** Synthesis and characterization of α-ZrP were performed according to the previously reported method.<sup>19,10</sup> In brief, α-ZrP was prepared by mixing Zr(IV)OCl<sub>2</sub> solution with phosphoric acid (9 M) followed by heating at 70 °C for 24 h. The resulting white crystalline solid was filtered, washed with acetone, and dried. X-ray powder diffraction data showed crystalline material with layer spacing of 7.6 Å.

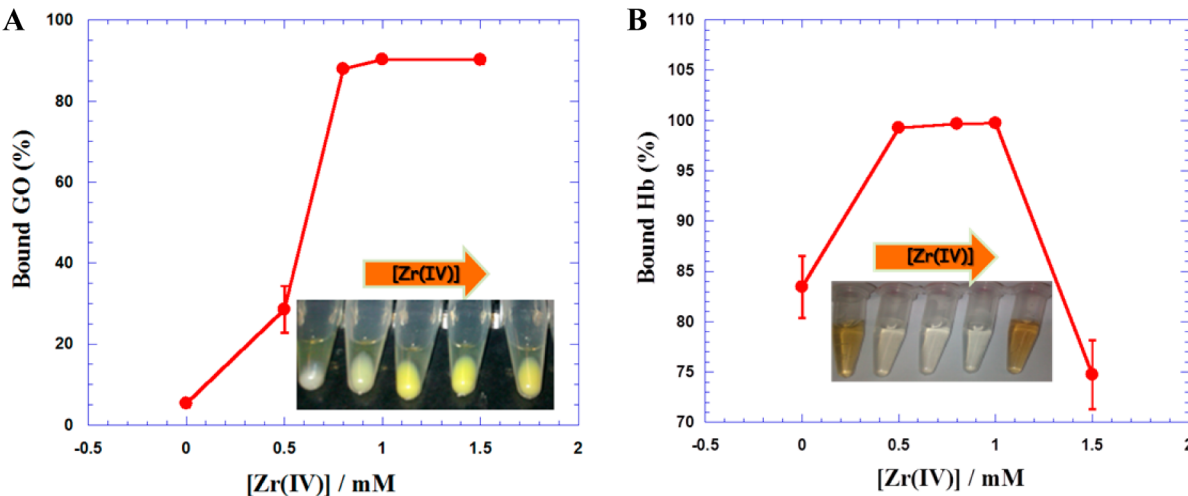


**Figure 1.** (A) Binding of GO (20  $\mu\text{M}$ ) and Hb (50  $\mu\text{M}$ ) to  $\alpha$ -ZrP (3 mM) as a function of the added Zr(IV) ion concentration (0–1.5 mM) in DI water, at room temperature. The color of  $\alpha$ -ZrP changed from white to light yellow due to the binding of GO, after centrifugation, as indicated in the inset photograph. (B) Enhanced binding of Hb to  $\alpha$ -ZrP by Zr(IV) and binding inhibition at higher concentrations. The color change of the supernatant accompanying Hb binding is shown in the inset picture. Error bars on some points are too small to be visible.

**2.2. Exfoliation and Enzyme Intercalation.** Stacks of  $\alpha$ -ZrP plates were exfoliated using tetrabutylammonium (TBA),<sup>41</sup> and the nanodiscs were exposed to desired enzyme-metal solutions at pH 3, which ultimately resulted in the formation of enzyme/metal/ $\alpha$ -ZrP intercalates. The layer spacing increased when enzymes were intercalated in  $\alpha$ -ZrP, as monitored by powder X-ray diffraction. The layer spacing increased from 7.6  $\text{\AA}$  for  $\alpha$ -ZrP to 16  $\text{\AA}$  for TBA/ $\alpha$ -ZrP, and these further increased to  $\sim$ 60  $\text{\AA}$  when GO or Hb was bound to the solid in the presence of 1 mM Zr(IV). In the case of Hb, we observed the second order diffraction peak at 31  $\text{\AA}$ , and this value is consistent with the layer spacing reported earlier for Hb/ $\alpha$ -ZrP of 64  $\text{\AA}$ .<sup>16</sup>

**2.3. Binding Studies.** Protein binding to exfoliated  $\alpha$ -ZrP nanodiscs was determined in the absence or the presence of specific metal ions at constant concentration of metal ion (1 mM) and  $\alpha$ -ZrP (3 mM), but at increasing concentrations of the protein. The concentration of metal ion was chosen such that there is substantial binding of the protein to the solid but the protein remained in solution. In other words, the metal did not precipitate the protein, under our experimental conditions. Since the pH of  $\text{ZrOCl}_2$  (1 mM) solution was 3, we chose this pH in control studies (H(I)) to account for the pH effect (pH adjusted using dilute HCl). Metal ion, protein and  $\alpha$ -ZrP mixtures were equilibrated for 30 min and centrifuged at 10 000 rpm for 5 min in a Fisher Scientific microfuge, Acspin micro 17 to separate the free enzyme from the bound. Concentration of free protein in the supernatant was determined by monitoring GO absorbance at 280 nm using the corresponding extinction coefficients ( $\epsilon = 1.336 \times 10^5 \text{ M}^{-1} \text{ cm}^{-1}$ ) or Hb absorbance at 406 nm ( $\epsilon = 3.397 \times 10^5 \text{ M}^{-1} \text{ cm}^{-1}$ ). Binding isotherms were constructed from these data and analyzed using Scatchard eq 1.<sup>42</sup> In eq 1,  $K_b$ ,  $n$ ,  $r$ , and  $c_f$  are the binding constant, the number of binding sites, binding density (ratio of the concentration of the bound enzyme to the concentration of  $\alpha$ -ZrP), and concentration of free enzyme, respectively. The Scatchard model is designed to quantify the interaction of an identical set of ligands to noninteracting, identical, nonoverlapping binding sites on a protein. This single-set of identical binding sites model is often used as a simplistic model to examine the binding of proteins to solid surfaces, and any deviations from the model is indicated by poor fits of the data to eq 1. Best fits to the data by nonlinear least-squares analysis resulted in the corresponding binding parameters. All conditions for the binding studies with specific metal ions are collected in Supporting Information Tables S1 and S2.

$$r/c_f = k_b(n - r) \quad (1)$$

**2.4. Zeta Potential Studies.** Laser doppler velocimetry was used to measure the zeta potentials on a Brookhaven Zeta Plus zeta potential analyzer. Sample suspensions (1.5 mL, 3 mM  $\alpha$ -ZrP) in deionized water were prepared, and pH adjusted to 3.0 using dilute HCl. The sample was transferred to a 4 mL polystyrene cuvette (Fisher Scientific). The zeta potential values were obtained by the Smoluchowski fit by software supplied by the manufacturer, and zeta potentials were calculated from the corresponding electrophoretic mobilities of the samples. Samples were equilibrated with the appropriate amounts of the metal salt, protein, and exfoliated  $\alpha$ -ZrP for 30 min at 25 °C, prior to the measurements.

**2.5. Activity Studies.** Activities were measured by suitable modification of published protocols, and activities of the ternary complexes have been compared with those of the corresponding binary complexes as well as untreated enzymes, under similar conditions of buffer, temperature, pH, and ionic strength. The enzyme/metal/ $\alpha$ -ZrP complexes were resuspended in 10 mM Tris HCl buffer pH 7.0 for activity studies at 25 °C. In a typical GO assay,<sup>43</sup> 2-methoxyphenol (10 mM), HRP (2  $\mu\text{M}$ ), glucose (0.2 mM), and GO (1  $\mu\text{M}$ ) were used. The hydrogen peroxide generated by the reduction of oxygen, coupled with the oxidation of glucose, reacts with 2-methoxyphenol, catalyzed by HRP, to produce a colored product, which has an absorption maximum at 470 nm. Kinetic data were plotted using Kaleida Graph (version 3.0), and the initial data points (0–30 s) were used to calculate the initial velocities and specific activities.

In a typical Hb assay, 2-methoxyphenol (2.5 mM in 10 mM Tris HCl buffer at pH 7.0) and  $\text{H}_2\text{O}_2$  (1.0 mM in DI) were added to Hb (1  $\mu\text{M}$  in 10 mM Tris HCl buffer at pH 7), and product formation was monitored at 470 nm as a function of time.<sup>44</sup> The initial velocities and the specific activities were calculated from the kinetic curves, as described above.

**2.6. Transmission Electron Microscopy (TEM) and X-ray Diffraction (XRD) Studies.** A carbon-coated Cu grid (400-mesh) was treated with plasma (Harrick PDC-32G) and coated with 1 mg/mL BSA solution. Aliquots of 3  $\mu\text{L}$  of 0.5 mM  $\alpha$ -ZrP were incubated on the grid for 1 h to allow particle adhesion. The grids were dried for 1 h and then moved directly to the microscope for imaging. For the imaging of enzyme/metal/ $\alpha$ -ZrP complexes, 3  $\mu\text{L}$  of mixture was applied where the protein concentration was 0.2 mg/mL and metal was 10  $\mu\text{M}$ . All the imaging has been done with FEI Tecnai Spirit transmission electron microscope with an operating voltage of 80 kV. The micrographs were recorded in a 4 megapixel AMT camera and presented as they are. The size bars for representative structures were drawn for clarity.

Suspensions of protein/Zr(IV)/ $\alpha$ -ZrP (2 mL) were spotted on glass slides and air-dried. XRD analysis of the samples was carried out with a Scintag model 2000 diffractometer using nickel-filtered CuK $\alpha$  radiation. Scan rates for these runs were 2°/min. The interlayer distances were measured from the 00l reflections ( $l = 1, 2, \text{etc.}$ ) using Bragg's law.

**2.7. Circular Dichroism (CD) Studies.** The CD spectra were recorded on a Jasco J-710 CD spectrometer using 1  $\mu\text{M}$  GO or 2  $\mu\text{M}$  Hb, 0.05 or 0.1 cm path length quartz cuvette from 260 to 190 nm, and a 1 cm cuvette has been used for recording the Soret CD spectra from 380 to 450 nm. Other operating parameters were as follows: sensitivity 20 mdeg, bandwidth 1.0 nm, response time 4 s, resolution 0.5 nm, speed 50 nm/min, and average of 3 scans. The CD spectra were corrected by subtracting the buffer signal, and data have been normalized as ellipticity per micromolar enzyme per unit path length.

### 3. RESULTS

In simple terms, the assembly of negatively charged proteins on negatively charged solid is feasible when excess negative charge at the protein–solid junction is neutralized by the sequestration of appropriate metal ions (Scheme 1). Explicit binding studies are carried out here to test this mechanistic model, using particular metal ions. Among the cations used here, Zr(IV) is the most acidic; the 1 mM solution in water had pH 3, and hence, binding studies with all other metal ions were carried out at pH 3. Details of our studies are enumerated below.

**3.1. Effect of Zr(IV) on Protein Binding.** The stacks of  $\alpha$ -ZrP were exfoliated by exposure to stoichiometric amounts of tetrabutylammonium hydroxide (TBA) and exposed to appropriate enzyme/metal ion mixtures (Scheme 1). The metal ion concentrations and protein concentrations were chosen such that the proteins did not precipitate in the presence of the added metal ion. At each metal ion concentration, bound protein concentration has been determined in centrifugation studies (Figure 1).

GO did not bind to  $\alpha$ -ZrP substantially, in the absence of Zr(IV), and binding increased from ~5% to ~90% at 0–1.0 mM [Zr(IV)] (Figure 1A). Further addition of the metal had no effect on binding, and after centrifugation of the samples the GO/Zr(IV)/ $\alpha$ -ZrP appeared as yellow precipitates (inset in Figure 1A). In the absence of  $\alpha$ -ZrP, the metal did not precipitate the protein, under any of these conditions.

Encouraged by the above findings, we tested if this strategy would also enhance the binding of moderately negatively charged Hb (pI 6.7). Hb (80  $\mu\text{M}$ ) binding to  $\alpha$ -ZrP (3 mM) increased from ~85 to 100% by the addition of Zr(IV) (0–0.5 mM), reached a plateau (1 mM Zr(IV)), and further addition (>1 mM) inhibited Hb binding altogether (Figure 1B). Under these conditions, Zr(IV) did not precipitate Hb, and binding inhibition above 1 mM Zr(IV) is not due to Hb precipitation. Zr(IV) may compete and displace Hb from the surface. The colors of the supernatants of Hb/Zr(IV)/ $\alpha$ -ZrP mixtures after centrifugation, as a function of increasing Zr(IV) concentration, are shown in the inset in Figure 1B. Hb binding to  $\alpha$ -ZrP was also promoted by Zr(IV), but not as dramatically as with GO because of the high affinity of Hb in the absence of Zr(IV), and binding saturated at 100%, even at high protein concentration (80  $\mu\text{M}$ ) and low metal ion concentration (0.5 mM).

**3.2. Effect of Other Metal Ions on the Binding Affinities.** Encouraged by the facile, Zr(IV)-mediated, binding of both GO and Hb to  $\alpha$ -ZrP, next we tested if this metal-promoted binding is unique to Zr(IV). The binding of GO (20  $\mu\text{M}$ ) to  $\alpha$ -ZrP (3 mM) was monitored in the presence of Cr(III), Ca(II), Mg(II), Na(I), and H(I) (1 mM cations, pH

3), and compared the data with that of Zr(IV)-mediated binding (Figure 2A, right bars). Ca(II) improved GO binding

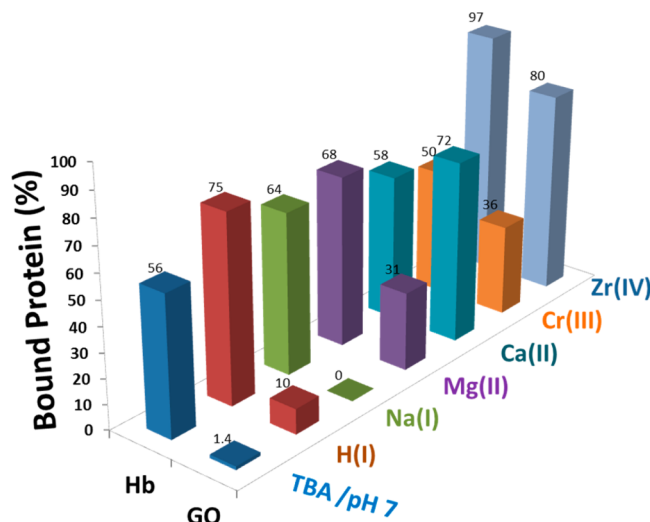


**Figure 2.** Binding of GO (20  $\mu\text{M}$ ) and Hb (80  $\mu\text{M}$ ) to  $\alpha$ -ZrP (3 mM) as a function of specific metal ions (1 mM, pH 3), as marked. Data in the absence of added metal ion were obtained at pH 7, and Cr(III) data are corrected for a small amount of protein precipitation by the metal ion.

substantially (~70%), slightly less than that of Zr(IV) (80%), but much better than Cr(III) (~35%); Mg(II) improved GO binding by ~30%, while Na(I) had essentially no measurable effect.

H(I) (pH 3) improved GO binding marginally (10%) but it was much better than that by Na(I) and highlights the weak role of pH in GO binding to  $\alpha$ -ZrP. The role of H(I) depends on the  $pK_a$  values of the specific functional groups at the interface, protonation and deprotonation, while the role of Na(I) depends on its binding/dissociation at the interface. H(I) and Na(I), having the same charge, served to evaluate specific roles of these ions in the binding process. Au(III), Al(III), Zn(II), Cu(II) and Ni(II) precipitated the protein even at pH 3, and could not be used for binding studies. The metal-mediated GO binding (1 mM metal ion, pH 3) followed the trend, Zr(IV) > Ca(II) > Cr(III) > Mg(II) > H(I) > Na(I), which indicated that the metal ion charge is not the absolute criterion to predict the ability of metal ions to promote protein binding.

Intrigued by the above unexpected trend, we examined the role of the protein by replacing strongly anionic GO by a more moderately anionic Hb. Hb (80  $\mu\text{M}$ ) binding to  $\alpha$ -ZrP (3 mM, pH 3) was also influenced by metal ions and the corresponding binding data are shown in Figure 2 (left bars) for comparison with those of the corresponding GO data.

One major difference between GO and Hb is that Hb binds to  $\alpha$ -ZrP with moderate affinity (56% binding, 80  $\mu\text{M}$  Hb, 3 mM  $\alpha$ -ZrP, pH 7), even in the absence of added metal ions (Figure 2). However, the binding was essentially quantitative (97%) in the presence of 1 mM Zr(IV). When compared to data in Figure 1, the Hb concentration in this experiment was increased to 80  $\mu\text{M}$ , so that there will be a substantial amount of free protein available for metal-promoted binding. Zr(IV) enhanced the loading capacity of Hb to 1:38 (protein to phosphate) mole ratio or 400% w/w. Such high loadings of

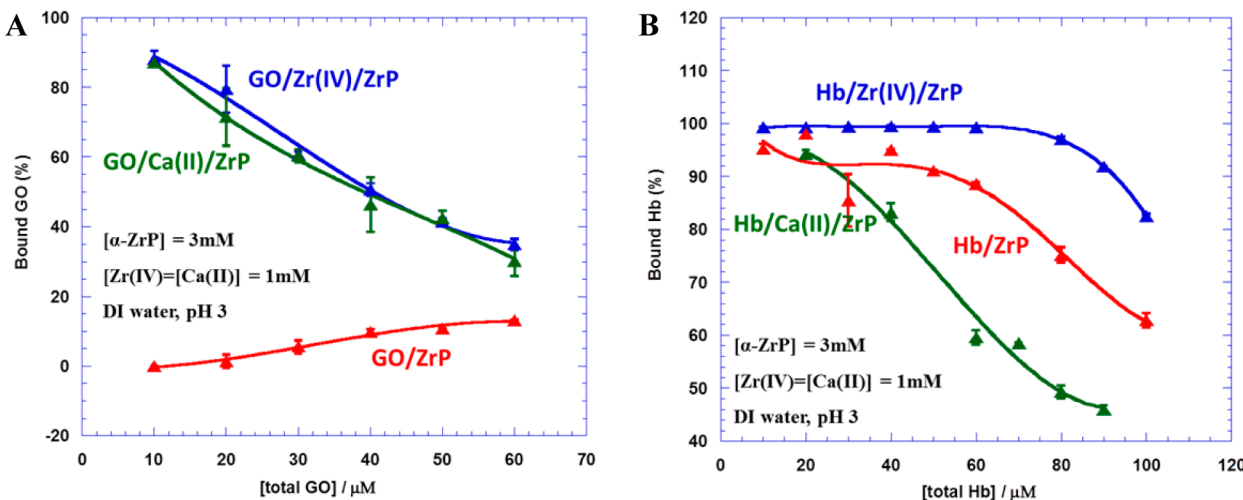


**Figure 3.** Binding isotherms of GO (A) and Hb (B), percent bound protein as a function of total protein concentration at a constant Zr(IV) (blue curves), Ca(II) (green curves), and H(I) (red curves) concentration (1 mM) and constant  $\alpha$ -ZrP (3 mM) at pH 3.

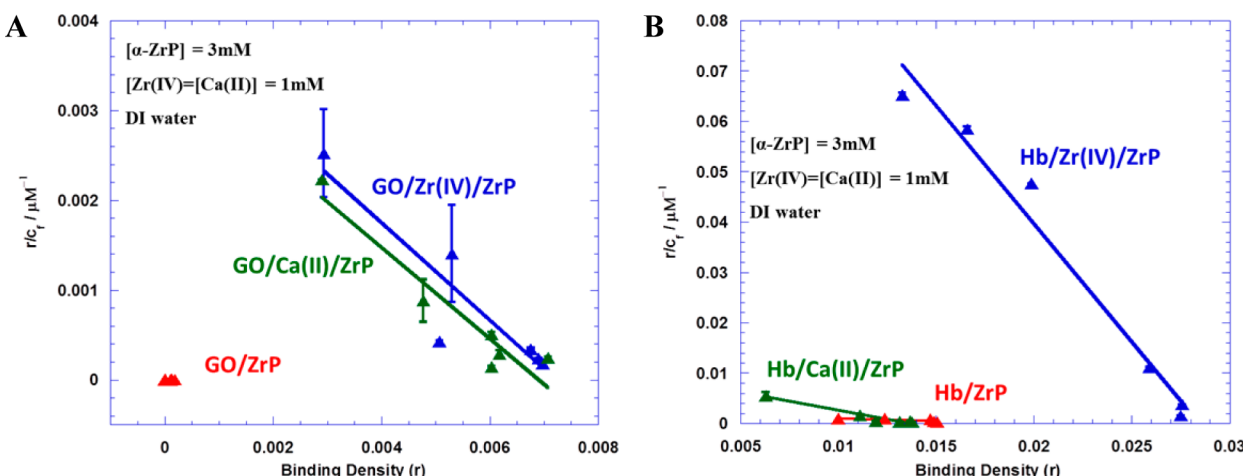


**Figure 4.** Scatchard plots in the presence of Zr(IV) (1 mM) (blue triangles), Ca(II) (green triangles), and H(I) (red triangles) for the binding of (A) GO and (B) Hb to  $\alpha$ -ZrP (3 mM, pH 3). The error bars on some points are too small to be visible.

proteins are rare to achieve and high loadings of the biocatalyst are advantageous for catalytic applications.

The next best promoter of Hb binding among all ions tested here was H(I), and this is primarily because Hb is strongly positively charged at pH 3 (pI 7). Hb affinity improved at pH 3 (75%) when compared to binding at pH 7 (56%), while all cations, except Zr(IV), did not exceed the effect of H(I), and Hb binding followed the order Zr(IV) > H(I) > Mg(II) > Na(I) > Ca(II) > Cr(III). Thus, H(I) is more effective than the trivalent Cr(III), which suggests that charge is not the primary criterion. Ca(II), which promoted the binding of GO strongly, had no such effect on Hb. Thus, the metal ion effect on the binding depended on the protein as well as the metal ion.

### 3.3. Effect of Protein Concentration on Binding.

Improved binding of both GO and Hb to  $\alpha$ -ZrP by added metal ions prompted us to quantify the binding constants. Binding studies were carried out at constant metal (1 mM) and  $\alpha$ -ZrP (3 mM) concentrations, while varying the protein concentration (Figure 3) at pH 3.

In the presence of Zr(IV) or Ca(II), as observed above, GO exhibited high percent of binding and nearly 90% binding has been achieved at low GO concentration ( $10 \mu\text{M}$ ) and 1 mM Zr(IV) (Figure 3A, blue triangles). Even at the highest GO

concentration ( $60 \mu\text{M}$ ), 58% of GO was still bound, or 100% w/w (GO to  $\alpha$ -ZrP), and the amount of bound protein increased steadily with the increase in protein concentration. These data were compared with the isotherms obtained in the presence of Ca(II) (green triangles) and H(I) (red triangles) (Figure 3A). Isotherms for Ca(II) and Zr(IV)-mediated GO binding are nearly the same, but these indicated higher loading than that of H(I).

The binding isotherm with Mg(II) indicated a similar effect as H(I) (Supporting Information Figure S1A, black triangles), but Na(I) had essentially no effect (green triangles). Binding isotherms with Cr(III) could not be obtained because of extensive protein precipitation by Cr(III) at  $>20 \mu\text{M}$  GO.

We also quantified the binding of Hb to  $\alpha$ -ZrP in the presence of Zr(IV) to construct the corresponding binding isotherms, and the data are shown in Figure 3B. Nearly 100% of Hb was bound in the presence of Zr(IV) (1 mM),  $\alpha$ -ZrP (3 mM), and this continued up until  $80 \mu\text{M}$  Hb, and then the percent binding began to decrease ( $100 \mu\text{M}$  Hb). Highest loading of Hb ( $80 \mu\text{M}$  Hb, 400% w/w Hb to  $\alpha$ -ZrP) was obtained with Zr(IV), which is nearly twice as much as that of Ca(II) but better than that of H(I).

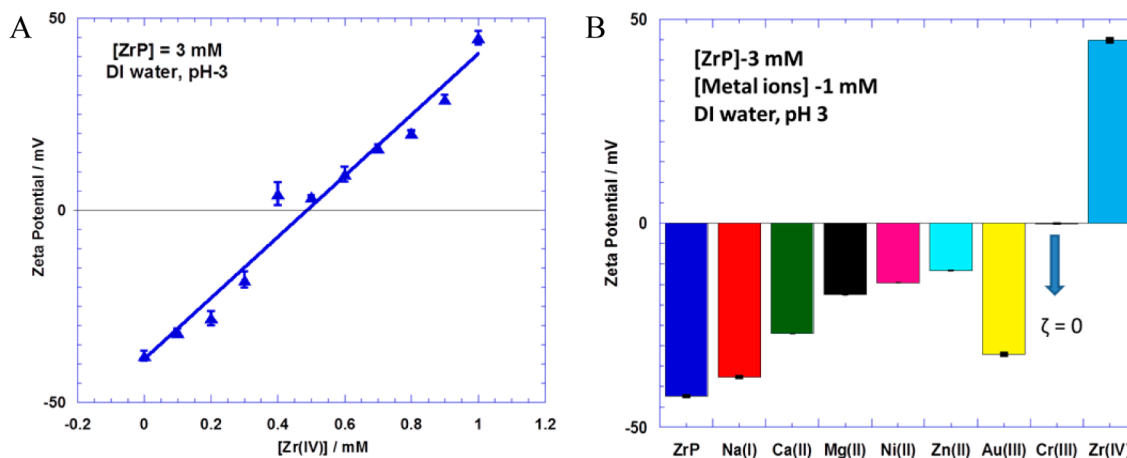


**Figure 5.** Zeta potential of exfoliated  $\alpha$ -ZrP nanosheets (A) as a function of  $[Zr(IV)]$  at pH 3 and (B) as a function of specific metal ions (1 mM) at pH 3.0, 25 °C.

The binding isotherms of Hb depended on the type of cation used (Supporting Information Figure S1B), as in the case of GO. At low Hb concentrations, all cations promoted binding substantially ( $\sim 100\%$ ), nearly equally, but the differences are clearer at higher Hb concentrations. At 80  $\mu$ M Hb, for example, the order of binding was  $Zr(IV) > H(I) > Mg(II) > Na(I) > Ca(II)$ , where  $Zr(IV)$  nearly doubled Hb loading on  $\alpha$ -ZrP.

**3.4. Binding Constants.** The above data were analyzed using the single, identical binding site model (Scatchard analysis), and the corresponding binding plots have been obtained for GO and Hb with  $Zr(IV)$ ,  $Ca(II)$ , and  $H(I)$  (Figure 4). The Scatchard plot of GO obtained in the presence of 1 mM  $Zr(IV)$  was linear (Figure 4A), and the best fit to eq 1 yielded a  $K_b$  of  $5.4 \times 10^5 \text{ M}^{-1}$  and a binding site size of 140 phosphates per GO. Six data points were used to calculate the binding constant, and the  $R$  value is 0.95. Almost the same results were obtained for  $Ca(II)$  with a binding constant of  $5.1 \times 10^5 \text{ M}^{-1}$ . In the absence of  $Zr(IV)$ , the binding of GO was too weak to obtain a good Scatchard plot, but the best estimate was  $0.014 \times 10^5 \text{ M}^{-1}$  (pH 3). GO binding affinity was enhanced  $\sim 380$ -fold by both  $Zr(IV)$  or  $Ca(II)$  (1 mM). The binding of a large ligand such as a protein with a solid surface involves multipoint versus multipoint binding, and the Scatchard analysis is too simplistic a model. The Scatchard model appears to be valid here, as indicated from the above reasonable linear fits to eq 1 in Figure 4, and validity of such an analysis can be understood in terms of the assumption that the protein functions as a single binding domain and that the entire binding site on the solid functions as a single integral binding site. This simplistic treatment is not unique to the current systems, and it has been widely noted earlier.<sup>11–18</sup>

In contrast to the high affinity binding of GO, the binding constant of Hb increased only  $\sim 40$ -fold from  $1.08 \times 10^5 \text{ M}^{-1}$  ( $H(I)$ ) to  $4.7 \times 10^6 \text{ M}^{-1}$  by  $Zr(IV)$  (Figure 4B), and the number of phosphates occupied per Hb decreased from  $\sim 50$  to  $\sim 35$ , thus enhancing the affinity and capacity. In case of Hb binding data, six data points were used to calculate the binding constants and the  $R$  value was 0.88.  $Ca(II)$  did not have any effect on the binding constant of Hb, nearly the same as that with  $H(I)$  (Supporting Information Figure S2). The binding plots with other metal ions were also obtained (Supporting Information Tables S1 and S2), and the binding constants varied in the order  $Zr(IV) \gg Mg(II) > Na(I) > Ca(II) > H(I)$  while the binding site sizes ( $n$ ) varied from 35 to 60 phosphates

per Hb. The maximal loading of Hb (400%) was nearly twice as that observed with GO (200%).

**3.5. Zeta Potential Studies.** The above data indicated the strong role of metal ions in protein binding to  $\alpha$ -ZrP, and we examined metal binding to  $\alpha$ -ZrP nanosheets by zeta potential measurements, which provides the average charge of the suspended particles. The binding of metal ions to  $\alpha$ -ZrP nanosheets is expected to lower its negative charge, and hence, zeta potential would be a direct measure of metal binding to the phosphate groups of the  $\alpha$ -ZrP nanosheets (phosphophilicity).

The charge of exfoliated  $\alpha$ -ZrP (3 mM) at pH 3 was  $-42 \pm 3$  mV, for example, and it linearly increased with the addition of  $Zr(IV)$ , reached zero at 0.4 mM  $Zr(IV)$  and further addition increased to  $+45 \pm 4$  mV at 1 mM  $Zr(IV)$ , Figure 5A). This charge variation and charge reversal is a direct evidence of  $Zr(IV)$  binding to  $\alpha$ -ZrP nanosheets, even at these low mM concentrations of  $Zr(IV)$ . Zeta potential measurements, therefore, were used to compare the relative affinities of specific metal ions (1 mM) to  $\alpha$ -ZrP (Figure 5B) where some metal ions are much more effective in lowering its negative charge or imparting it a net positive charge. The net charge on  $\alpha$ -ZrP nanosheets followed the order,  $Zr(IV) \gg Cr(III) > Zn(II) > Ni(II) > Mg(II) > Ca(II) > Au(III) > Na(I)$ , a direct measure of the relative phosphophilicities of these metal ions. Despite the high charge,  $Au(III)$  is a poor binder to  $\alpha$ -ZrP, while  $Cr(III)$  is much better than all other metal ions, except  $Zr(IV)$ . The divalent metal ions differed substantially, in terms of their affinities for  $\alpha$ -ZrP and  $Zn(II)$  showed the highest affinity while  $Ca(II)$  had the lowest. Thus, metal binding to  $\alpha$ -ZrP can not be predicted solely based on metal ion charge.

Zeta potential measurements were also useful to follow the binding of proteins to  $\alpha$ -ZrP (Supporting Information Figure S3A and B). The gradual addition of GO (up to 6  $\mu$ M GO) to a mixture of  $Zr(IV)$  (1 mM) and  $\alpha$ -ZrP (3 mM, pH 3) decreased the charge from  $+45 \pm 4$  mV to  $\sim +20 \pm 4$ , and then there was no significant change with further increase in protein concentration. In the case of Hb, charge decreased almost linearly with protein concentration from  $+45 \pm 4$  to  $\sim +16.0 \pm 4$  mV (Supporting Information Figure S3B). The charges on specific protein/metal/ $\alpha$ -ZrP complexes were also compared (Supporting Information Figure S3C), and zeta potentials followed the order:  $Zr(IV)/\alpha$ -ZrP > GO/ $Zr(IV)/\alpha$ -ZrP > Hb/ $Zr(IV)/\alpha$ -ZrP > Hb/ $\alpha$ -ZrP > GO/ $\alpha$ -ZrP >  $\alpha$ -ZrP. The metal/protein/ $\alpha$ -ZrP complexes had a net positive charge, lower than

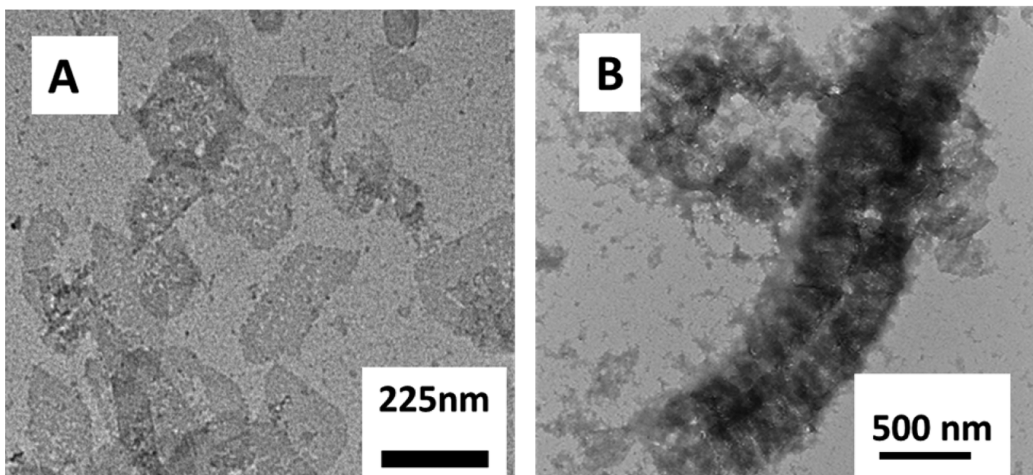


**Figure 6.** TEM images of exfoliated  $\alpha$ -ZrP (A) and GO/Zr(IV)/ $\alpha$ -ZrP (0.2 mg/mL GO, 0.01 mM Zr(IV), 0.5 mM  $\alpha$ -ZrP) (B) indicated the layered structures of the metal enzyme assemblies in  $\alpha$ -ZrP on a micrometer scale.

that of Zr(IV)/ $\alpha$ -ZrP, which indicated charge neutralization by protein binding; while the protein/ $\alpha$ -ZrP complexes had a net negative charge, lower than that of  $\alpha$ -ZrP, which also indicated charge neutralization by protein binding. We observe that there was an average drop of +20 mV after protein binding to metal/ $\alpha$ -ZrP, and an average drop of -25 mV of charge due to protein binding to  $\alpha$ -ZrP. Both these opposing observations indicate charge reduction, which can be explained only if ions are released/absorbed during protein binding.

**3.6. TEM Studies.** Morphology studies were carried out to confirm the assembly of GO in  $\alpha$ -ZrP galleries in the presence of Zr(IV). The micrographs of exfoliated  $\alpha$ -ZrP showed nanosheets of 200–300 nm in size (Figure 6A) while GO/Zr(IV)/ $\alpha$ -ZrP (Figure 6B) formed elongated, uniform stacks of several micrometers in length, which is quite surprising. Previously, powder XRD studies showed that exfoliated  $\alpha$ -ZrP plates reassemble back to the layered structure after enzyme binding.<sup>23</sup> But the neat, ordered arrangement was rarely seen in the TEM or SEM images after protein intercalation. The formation of long strands of metal/enzyme/inorganic strands of over a micrometer length and about half a micrometer in diameter are novel features of these materials.

The powder XRD also confirmed the TBA/ $\alpha$ -ZrP stacks (a sharp peak at 16.9 Å) (Supporting Information, Figure S4), as reported earlier.<sup>22</sup> Layered structures of protein/Zr(IV)/ $\alpha$ -ZrP are observed. The TEM data, combined with the powder XRD, confirm that proteins intercalate between the layers of  $\alpha$ -ZrP, and these appear to form large self-assembled structures.

**3.7. Enzyme Structure Retention and Activities of the Bound Enzymes.** One very important aspect of a biocatalyst is that it should have substantial structure retention and activity. Circular dichroism (CD) studies are used to examine the extent of retention of protein structure in the above assemblies. The far UV CD spectra of the samples are recorded in the 190–260 nm region and compared with those of free proteins (Supporting Information Figure S5). Data showed that the CD spectra of GO and Hb are distorted to some extent by the metal ions, but this distortion is relieved in the case of Cr(III), on binding to  $\alpha$ -ZrP.

The loss of structure was a concern, and we examined this aspect by quantitating the oxidase and peroxidase activities of the bound GO and Hb, respectively. The GO/metal/ $\alpha$ -ZrP

biocatalysts are suspended in phosphate buffer, and kinetic traces were followed as a function of time (Supporting Information Figures S6, S7). The initial rates of the reaction were obtained from the slopes of the kinetic plots at early times, and the corresponding specific activities shown in Figure 7.

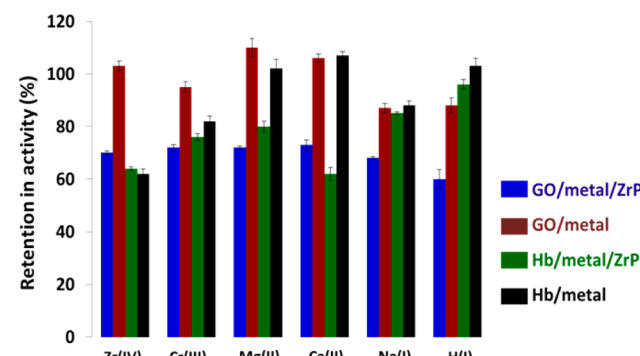


**Figure 7.** Comparison of the percent retention of enzyme activities for GO (1  $\mu$ M) bound to  $\alpha$ -ZrP (0.2 mM), 0.1 mM metal in 10 mM Tris-HCl buffer at pH 7.0 at room temperature, and Hb (1  $\mu$ M) bound to  $\alpha$ -ZrP (0.06 mM) in 10 mM Tris-HCl buffer at pH 7.0 at room temperature. The kinetic traces of the activity assays (absorbance vs time) for different systems are (Supporting Information Figures S6 and S7) used to determine the initial rates and specific activities.

Specific activities of GO samples are normalized with respect to that of free GO as 100% and those of Hb samples with respect to that of free Hb as 100%. The relative activities of the GO/metal (brown bars) or GO/metal/ $\alpha$ -ZrP (blue bars) varied from 70 to 100% (Figure 7, Supporting Information Figures S6 and S7). Zr(IV), Cr(III), Mg(II), and Ca(II) did not have substantial effect on GO activity, and all GO/metal/solid assemblies had nearly same specific activities. The specific activity of GO/Zr(IV)/ $\alpha$ -ZrP ( $6.1 \times 10^{-3} \text{ M}^{-1} \text{ s}^{-1}$ ) is essentially the same as that of GO/H(I)/ $\alpha$ -ZrP ( $5.7 \times 10^{-3} \text{ M}^{-1} \text{ s}^{-1}$ , under the same conditions). While metal ions have increased affinities and improved loadings, they did not adversely influence GO activities.

Along these lines, specific activities of Hb/metal/ $\alpha$ -ZrP (green bars) and Hb/metal (black bars) are compared under the same conditions (Figure 7). Hb/Zr(IV)/ $\alpha$ -ZrP activity (3.6

$\times 10^{-4} \text{ M}^{-1} \text{ s}^{-1}$ ) is slightly lower than that of Hb/H(I)/ $\alpha$ -ZrP ( $5.4 \times 10^{-4} \text{ M}^{-1} \text{ s}^{-1}$ ). Activities of Hb/metal/ $\alpha$ -ZrP followed the order H(I) > Na(I) > Mg(II) > Cr(III) > Ca(II)  $\simeq$  Zr(IV).

#### 4. DISCUSSION

The role of metal ions in the binding of proteins to  $\alpha$ -ZrP nanodiscs is tested here, and the binding resulted in protein intercalation into the galleries. The binding, morphology, structure, and activities indicated that Zr(IV) and Ca(II) functioned as excellent metal glues to enhance protein binding and loading. Ca(II) increased the binding affinity of GO but not that of Hb. These observations are consistent with the proposed ICPB mechanism for the binding of anionic proteins to anionic  $\alpha$ -ZrP.

GO is negatively charged at neutral pH ( $\text{pI} \sim 4$ ),<sup>30</sup> and its affinity for the negatively charged  $\alpha$ -ZrP is poor even at pH 3. According to the ICPB mechanism, sequestration of appropriate cations at the protein–solid interface facilitates binding by promoting charge neutralization at the interface. Current data show that 1 mM Zr(IV) or Ca(II) essentially increase GO binding (20  $\mu\text{M}$  GO) to  $\alpha$ -ZrP (3 mM, pH 3) from essentially zero to 90%, and enhancements depended on the protein concentration as well as the metal concentration. Increased affinity was not at the expense of activities, as indicated by the activity studies.

The affinity increases depended on the type of metal ion as well as the nature of the protein. Metal ions that bind tightly to the solid as well as the protein are expected to be the best metal glues. Zeta potential studies indicated that the relative affinities of the metal ions for the nanosheets followed the trend, Zr(IV)  $\gg$  Cr(III) > Zn(II) > Ni(II) > Mg(II) > Ca(II) > Au(III) > Na(I) > H(I) which is related to their relative phosphophilicities. Zr(IV) is strongly oxophilic and its high affinity for the phosphate groups of  $\alpha$ -ZrP has been already demonstrated,<sup>31–34</sup> and current data are consistent with these reports.

Quantitative binding of Zr(IV) to exfoliated nanosheets of  $\alpha$ -ZrP was confirmed by the phenylphosphonic acid chelation assay, developed in our lab (Supporting Information, Figure S8). The amount of free [Zr(IV)] after equilibration with 1 mM  $\alpha$ -ZrP (pH 3) was determined, after separation by centrifugation followed by chelation with phenylphosphonic acid.

Zr(IV) has high formation constants with carboxylic and amine ligands,<sup>36,45,46</sup> and strong affinity of Zr(IV) for  $\alpha$ -ZrP may be combined with its high affinity for the carboxylic and/or amino groups of proteins to enhance protein binding to the solid by several orders of magnitude. The high charge density, large coordination number, and high phosphate affinity of Zr(IV) are responsible for its role as a metal-glue. The zeta potential data suggest that Cr(III) is also strongly phosphophilic, next to Zr(IV), but it is surprising that Au(III) had much poorer ability to neutralize  $\alpha$ -ZrP charge than anticipated.

Ca(II) was known to have a high affinity to  $\alpha$ -ZrP over any other divalent cations,<sup>37</sup> but zeta potential data show that it is not as good as Zn(II), Mg(II), or Ni(II), and this deviation is due to lower pH used here (pH 3). Ca(II) also improved protein binding much better than Mg(II), and protein binding studies with Zn(II) and Ni(II) could not be carried out due to precipitation issues. Note that Ca(II) is a better binder to the COOH/NH<sub>2</sub> groups of proteins than Mg(II). Thus, charge is not the only criterion for predicting the binding enhancement (Supporting Information Table S3). The ability of the metal to coordinate to the phosphate groups of the solid and/or to the

carboxyl/amino groups of the proteins is also important in assessing the efficacy of a metal ion in promoting protein binding to  $\alpha$ -ZrP.

Ca(II) promoted GO binding to  $\alpha$ -ZrP but not Hb, but Zr(IV) promoted binding of both proteins to  $\alpha$ -ZrP. Thus, metal-mediated binding depended on the protein. In the case of Zr(IV), both amino and carboxylic groups are known to coordinate to the metal, and it can complex with either the COOH-rich surface of GO or the COOH/NH<sub>2</sub>-rich surface of Hb or to the phosphate groups of  $\alpha$ -ZrP. Ca(II) may have higher specific affinity for GO than Hb due to the larger number of surface COOH groups on GO (132 per GO dimer, 1.7 carboxylic groups/nm<sup>2</sup> of protein surface) when compared to that of Hb (60 COOH groups per tetramer, 0.53 carboxylic groups/nm<sup>2</sup> of protein surface and 61 lysines per tetramer, 0.54 amino groups/nm<sup>2</sup> protein surface). The formation constants of amino or polyamino complexes of Ca(II) are small,<sup>40</sup> but the log *K* of polycarboxylic ligands with Ca(II) was 3–4 times higher than that with a simple acetate group.<sup>40</sup> So, we suspect that Ca(II) may bind better to the carboxyl-rich surfaces of GO than amine-rich surfaces of Hb.

Mg(II) was more effective in reducing the negative charge of  $\alpha$ -ZrP than Ca(II) (more phosphophilic), but its ability to promote GO binding to  $\alpha$ -ZrP was much less than that of Ca(II), and significantly less than Mg(II)-mediated binding of DNA to mica.<sup>12</sup> Both Mg(II) and Ca(II) complexes of phosphate and carboxylate ligands have comparable formation constants,<sup>40</sup> but binding of Mg(II) to proteins is weak.<sup>47</sup> To sum up, it is not just the charge of the cation that is important but its affinity for the functional groups decorating the protein surface, as well as the phosphate groups of  $\alpha$ -ZrP play an important role in promoting protein binding.

The average area occupied by GO at the highest loading is 3500 Å<sup>2</sup> as estimated from the maximum loading of 100% (w/w). This value is comparable to the cross-sectional area of GO (diameter of  $\sim$ 60 Å).<sup>25</sup> It points to a very tight packing of GO in the galleries, and this could be one reason that the activity of GO/Zr(IV)/ $\alpha$ -ZrP is lower than that of the free GO. Strong interactions and high loading may have resulted in the formation of metal/enzyme frameworks which appeared in the TEM images to be neatly arranged. The maximal loading of Hb was much greater than that of GO, 200% (w/w), and this is far greater than reported for any other protein or solid.

In general, the w/w binding capacities of a variety of solid surfaces rarely exceed 50%,<sup>48</sup> and one exception has been the loading of urease on a tentacle type polymer (100% w/w, enzyme to solid).<sup>49</sup> Compared to other supports,  $\alpha$ -ZrP is a promising solid platform for high protein loadings, when used in conjunction with suitable metal ions. This is because of the large number of phosphate groups per unit area of  $\alpha$ -ZrP (1 per  $\sim$ 25 Å<sup>2</sup>), and charge neutralization of the enzyme/solid interface may be a very important requirement for high loading. Enhanced binding density is important for biocatalytic applications where maximal loading of the catalyst per unit mass of the support matrix is beneficial. In support of these inferences,  $\alpha$ -ZrP has been reported to form multilayered self-assembled structures.<sup>20</sup> Formation of long strands of GO/Zr(IV)/ $\alpha$ -ZrP with near-perfect ordering of the plates is unusual, and this indicates the propensity for assembly formation.

Enzyme/metal/ $\alpha$ -ZrP materials retained significant activities, which are comparable to those of the corresponding enzyme/ $\alpha$ -ZrP binary complexes but less than those of the free enzymes.

The specific activities of GO/Zr(IV)/ $\alpha$ -ZrP and Hb/Zr(IV)/ $\alpha$ -ZrP are  $6.1 \times 10^{-3}$  and  $3.6 \times 10^{-4} \text{ M}^{-1} \text{ s}^{-1}$ , respectively, and these are comparable to those of the corresponding enzyme/ $\alpha$ -ZrP complexes ( $5.2 \times 10^{-3} \text{ M}^{-1} \text{ s}^{-1}$  for GO and  $5.4 \times 10^{-4} \text{ M}^{-1} \text{ s}^{-1}$  for Hb). Zr(IV) and Cr(III) inhibited specific activities of GO to a small extent, and this could be partly responsible for the reduction in the activities of the corresponding GO/metal/ $\alpha$ -ZrP materials. Activities of all GO/metal/ $\alpha$ -ZrP samples examined here are comparable to that of GO/H(I)/ $\alpha$ -ZrP, while activities of Hb/metal/ $\alpha$ -ZrP followed the trend H(I) > Na(I) > Mg(II) > Cr(III) > Ca(II)  $\approx$  Zr(IV). Higher affinities for the solid correlated with lower activities, with the exception of Hb/Na(I)/ $\alpha$ -ZrP. The tight packing of the proteins in the galleries, promoted by efficient charge neutralization by the added metal ions, could be one reason. Even so, the metal/enzyme/solid ternary complexes retained substantial activities, despite crowding in the galleries.

## 5. CONCLUSIONS

Metal ions, protons, counterions, water molecules, and others are to be considered in the adsorption of proteins on solid surfaces.<sup>16,22</sup> In particular, previous studies suggested that sequestration of cations is required to neutralize excess charge that could develop at the interface when a negatively charged enzyme binds to a negatively charged solid. Sharing of ions was also suggested when anionic biomolecules such as DNA bind to anionic solids such as mica where Mg(II) played a key role in charge neutralization. The strength of interaction depended on the charge density of the biomolecule, the solid, and the metal ion.<sup>50</sup> Here, we tested the role of specific cations in the binding of two model systems GO and Hb. One of the most exciting observations is that the binding affinities of both proteins are increased significantly by Zr(IV), primarily due to its strong phosphophilicity for the  $\alpha$ -ZrP surface and the carboxyl/amino surfaces of proteins. Zeta potential data show that Zr(IV) and Cr(III) are far better binders to  $\alpha$ -ZrP than all the other metal ions tested here. Out of these two proteins, GO is the highest negatively charged protein (charge  $> -80$  at pH 7, pI = 4, positively charged at pH 3) which showed highest metal-enhanced binding. On the other hand, Hb showed higher binding in the absence of metal and less metal-mediated binding (pI  $\sim$  6.7). Ca(II) promoted the binding of GO but not Hb, because of its moderate affinity for  $\alpha$ -ZrP but strong ability to coordinate to the carboxyl-rich GO surface but not the amine-rich Hb surface.

The increase in the affinity cannot be attributed to simple ionic strength effects or pH changes, although these do contribute to binding enhancements. Metal ion binding to the anionic  $\alpha$ -ZrP nanodiscs and to the enzyme surface contributes to the observed affinity increases. The ions with the highest charge, charge density, oxophilicity, and phosphophilicity (Zr(IV), Ca(II), H(I)) promoted the binding the most, while no correlation was noted with ion size, hydration, or charge density (Supporting Information Table S3). The proposition that cations may play a key role in the binding of these systems with  $\alpha$ -ZrP is confirmed, and for a given metal the extent of affinity increase depended directly on enzyme charge.

Consistent with this evaluation, we previously reported that when these anionic proteins are converted to the corresponding cationic derivatives by surface group modification, their binding affinities to  $\alpha$ -ZrP was increased by orders of magnitude.<sup>24</sup> Thus, these two approaches are parallel, complementary, and

they confirm the strong role of charge in the binding interactions.

High affinities are also accompanied by higher loading capacities, and this aspect is promising for biocatalytic applications; and suitable cations can enhance loading as well as binding affinities without compromising activities. To the best of our knowledge, the maximum loading of 400% w/w of any protein on any solid is the highest ever reported, and nearly the 400-fold increase in binding affinity of GO is also novel. Our conclusion is that metal ions provide new avenues to enhance binding of anionic proteins to anionic solids, when there are suitable functional groups on one or both partners for anchoring the cations.

TEM images show that the structure of the solid after immobilization is also conserved, and that metal ions promote the self-assembly of proteins and  $\alpha$ -ZrP nanosheets as long strands. Proteins generally do not tend to self-assemble, unless the unfavorable protein–protein repulsions are overcome by suitable means. Metal ions of appropriate charge density and solid surfaces serve to control these interactions and form macroscopic frameworks.

In addition to the effect on the binding, the metal ions also influenced the catalytic activities of the bound enzymes. This was not anticipated. Far UV CD data showed that the CD spectra of GO and Hb are distorted but this distortion is relieved to some extent, in the case of Cr(III), on binding to  $\alpha$ -ZrP (Supporting Information Figure S8). In the case of Zr(IV), the protein structure is distorted to a large extent, but an appreciable amount of activity is still retained and bound enzyme activities are comparable to those of the native enzymes. We conclude that carefully chosen cations can enhance the binding affinities of particular proteins by orders of magnitude without adversely affecting their activities, and this ability depends on their affinities for the solid as well as the proteins. These physical insights are important in the rational design of surfaces for benign, high affinity adsorption of proteins to solid surfaces.

## ■ ASSOCIATED CONTENT

### S Supporting Information

Electronic forms of powder XRD, circular dichroism spectra, binding isotherms, specific concentrations used for particular studies, some properties of cations, and binding parameters for the enzyme/cation/solid systems are given. This material is available free of charge via the Internet at <http://pubs.acs.org>.

## ■ AUTHOR INFORMATION

### Notes

The authors declare no competing financial interest.

## ■ ACKNOWLEDGMENTS

We thank the National Science Foundation (DMR, BMAT-1005609) for generous financial support of this work.

## ■ REFERENCES

- (1) Oohora, K.; Burazerovic, S.; Onoda, A.; Wilson, Y. M.; Ward, T. R.; Hayashi, T. Chemically Programmed Supramolecular Assembly of Hemoprotein and Streptavidin with Alternating Alignment. *Angew. Chem., Int. Ed.* **2012**, *51*, 3818–3821.
- (2) Erkelenz, M.; Kuo, C. H.; Niemeyer, C. M. DNA-Mediated Assembly of Cytochrome P450 BM3 Subdomains. *J. Am. Chem. Soc.* **2011**, *133*, 16111–8.

- (3) Yoshimatsu, K.; Lesel, B. K.; Yonamine, Y.; Beierle, J. M.; Hoshino, Y.; Shea, K. J. Temperature-Responsive "Catch and Release" of Proteins by using Multifunctional Polymer-Based Nanoparticles. *Angew. Chem., Int. Ed.* **2012**, *51*, 2405–2408.
- (4) Radford, R. J.; Tezcan, F. A. A Superprotein Triangle Driven by Nickel(II) Coordination: Exploiting Non-Natural Metal Ligands in Protein Self-Assembly. *J. Am. Chem. Soc.* **2009**, *131*, 9136–9137.
- (5) Munch, H. K.; Heide, S. T.; Christensen, N. J.; Jensen, T. H.; Thulstrup, P. W.; Jensen, K. J. Controlled Self-Assembly of Re-engineered Insulin by Fe(II). *Chem.—Eur. J.* **2011**, *17*, 7198–7204.
- (6) Brodin, J. D.; Ambroggio, I.; Tang, C.; Parent, K. N.; Baker, T. S.; Tezcan, F. A. Metal-directed, chemically tunable assembly of one-, two- and three-dimensional crystalline protein arrays. *Nat. Chem.* **2012**, *4*, 375–382.
- (7) Mulchandani, A.; Rogers, K. R. *Enzyme biosensors*, Part 1; Humana Press: New York, 1998.
- (8) Elnashar, M. M. M. Immobilized Molecules Using Biomaterials and Nanobiotechnology. *J. Biomater. Nanobiotechnol.* **2010**, *1*, 61–77.
- (9) Sharma, B. P.; Bailey, L. F.; Messing, R. A. Immobilized Biomaterials—Techniques and Applications. *Angew. Chem., Int. Ed.* **2003**, *21*, 837–854.
- (10) Chang, T. M. *Biomedical Applications of Immobilized Enzymes and Proteins*; Springer: New York, 1977; Vol. 1.
- (11) Mudhavarthi, V. K.; Bhamhani, A.; Kumar, C. V. Novel enzyme/DNA/inorganic nanomaterials: a new generation of biocatalysts. *Dalton Trans.* **2007**, 5483.
- (12) Hansma, H. G.; Laney, D. E. DNA Binding to Mica Correlates with Cationic Radius: Assay by Atomic Force Microscopy. *Biophys. J.* **1996**, *70*, 1933–1939.
- (13) Pastre, D.; Piétrement, O.; Fusil, S.; Landousy, F.; Jeusset, J.; David, M. O.; Hamon, L.; Cam, E. L.; Zozime, A. Adsorption of DNA to Mica Mediated by Divalent Counter ions: A Theoretical and Experimental Study. *Biophys. J.* **2003**, *85*, 2507–2518.
- (14) Guo, M.; Yang, W.; Coghill, L.; Campopiano, D. J.; Parkinson, J. A.; MacGillivray, R. T.; Harris, W. R.; Sadler, P. J. Synergistic anion and metal binding to the ferric ion-binding protein from Neisseria gonorrhoeae. *J. Biol. Chem.* **2003**, *24*, 2490–2502.
- (15) Alexeev, D.; Zhu, H.; Guo, M.; Zhong, W.; Hunter, D.; Yang, W.; Campopiano, D. J.; Sadler, P. A novel protein-mineral interface. *Nat. Struct. Biol.* **2003**, *10*, 297–302.
- (16) Kumar, C. V.; Chaudhari, A. Proteins Immobilized at the Galleries of Layered  $\alpha$ -Zirconium Phosphate: Structure and Activity Studies. *J. Am. Chem. Soc.* **2000**, *122*, 830–837.
- (17) Duff, M. R.; Kumar, C. V. Molecular Signatures of Enzyme–Solid Interactions: Thermodynamics of Protein Binding to  $\alpha$ -Zr(IV) Phosphate Nanoplates. *J. Phys. Chem. B.* **2009**, *113*, 15083–15089.
- (18) Duff, M. R.; Kumar, C. V. Protein–Solid Interactions: Important Role of Solvent, Ions, Temperature, and Buffer in Protein Binding to  $\alpha$ -Zr(IV) Phosphate. *Langmuir* **2009**, *25*, 12635–12643.
- (19) Clearfield, A.; Stynes, J. A. J. The preparation of crystalline zirconium phosphate and some observations on its ion exchange behaviour. *Inorg. Nucl. Chem.* **1964**, *26*, 117.
- (20) Clearfield, A.; Smith, G. D. Crystallography and structure of alpha-zirconium bis(monohydrogen orthophosphate) monohydrate. *Inorg. Chem.* **1969**, *8*, 431–436.
- (21) Kaschak, D. M.; Johnson, S. A.; Hooks, D. E.; Kim, H. N.; Ward, D. M.; Mallouk, T. E. Chemistry on the Edge: A Microscopic Analysis of the Intercalation, Exfoliation, Edge Functionalization, and Monolayer Surface Tiling Reactions of  $\alpha$ -Zirconium Phosphate. *J. Am. Chem. Soc.* **1998**, *120*, 10887–10894.
- (22) Kumar, C. V.; Bhamhani, A.; Hnatiuk, N. *Handbook of Layered Materials*; Carrado, K., Dutta, P., Auerbach, S., Eds.; Marcel Dekker: New York, 2004.
- (23) Agustin, D.; Saxena, V.; González, J.; David, A.; Casan, B.; Carpenter, B.; Batteas, J. D.; Colon, J. L.; Clearfield, A.; Hussain, M. D. Zirconium phosphate nano-platelets: a novel platform for drug delivery in cancer therapy. *Chem. Commun.* **2012**, *48*, 1754–1756.
- (24) Chowdhury, R.; Stromer, B.; Pokharel, B.; Kumar, C. V. Control of Enzyme–Solid Interactions via Chemical Modification. *Langmuir* **2012**, *28*, 11881–11889.
- (25) Wilson, R.; Turner, A. P. F. Glucose oxidase: an ideal enzyme. *Biosens. Bioelectron.* **1992**, *7*, 165–185.
- (26) Gibson, H. Q.; Swoboda, B. E. P.; Massey, V. Kinetics and Mechanism of Action of Glucose Oxidase. *J. Biol. Chem.* **1964**, *239*, 3927.
- (27) Periasamy, A. P.; Chang, Y. J.; Chen, S. M. Amperometric glucose sensor based on glucose oxidase immobilized on gelatin-multiwalled carbon nanotube modified glassy carbon electrode. *Bioelectrochem.* **2011**, *80*, 114–120.
- (28) Katz, E.; Willner, I. A. A Biofuel Cell with Electrochemically Switchable and Tunable Power Output. *J. Am. Chem. Soc.* **2003**, *125*, 6803–6813.
- (29) Smith, M. J.; Beck, W. S. Peroxidase activity of hemoglobin and its subunits: Effects thereupon of haptoglobin. *Biochim. Biophys. Acta, Protein Struct.* **1967**, *147*, 324–333.
- (30) Zubay, G. *Biochemistry*; W. C. Brown Publishing: TX, 1999.
- (31) Grant, K. B.; Kassai, M. Major Advances in the Hydrolysis of Peptides and Proteins by Metal Ions and Complexes. *Curr. Org. Chem.* **2006**, *10*, 1035–1049.
- (32) Guo, M.; Yang, W.; Coghill, L.; Campopiano, D. J.; Parkinson, J. A.; MacGillivray, R. T.; Harris, W. R.; Sadler, P. J. Synergistic anion and metal binding to the ferric ion-binding protein from Neisseria gonorrhoeae. *J. Biol. Chem.* **2003**, *24*, 2490–2502.
- (33) Hyun, P. J.; In-Ae, B.; Ho, C. S. Preparation of  $Zr^{4+}$  affinity column by atom transfer radical polymerization for phosphoprotein isolation. *J. Appl. Polym. Sci.* **2009**, *114*, 1250–1255.
- (34) Feng, S.; Ya, M.; Zhou, H.; Jiang, X.; Jiang, X.; Zou, H.; Cong, B. Immobilized zirconium ion affinity chromatography for specific enrichment of phosphopeptides in phosphoproteome analysis. *Mol. Cell. Proteomics* **2007**, *6*, 1656–1666.
- (35) Monot, J.; Petit, M.; Lane, S. M.; Guisle, I.; Léger, J.; Tellier, C.; Talham, D. R.; Bujoli, B. Towards Zirconium Phosphonate-Based Microarrays for Probing DNA-Protein Interactions: Critical Influence of the Location of the Probe Anchoring Groups. *J. Am. Chem. Soc.* **2008**, *130*, 6243–6251.
- (36) Mazur, M.; Krysiński, P.; Blanchard, G. J. Use of Zirconium-Phosphate-Carbonate Chemistry to Immobilize Polycyclic Aromatic Hydrocarbons on Boron-Doped Diamond. *Langmuir* **2005**, *21*, 8802–8808.
- (37) Clearfield, A.; Nancollas, G. H.; Blessing, R. H. *Ion Exchange and Solvent Extraction*; Marinsky, J. A., Marcus, Y., Eds.; Marcel Dekker, Inc.: New York, 1973; No. 5; pp 11, 119.
- (38) Toffaletti, J.; Gitelman, H. J.; Savory, J. Separation and quantification of serum constituents with calcium by gel filtration. *Clin. Chem.* **1976**, *22*, 1968–1972.
- (39) Black, C. B.; Huang, H. W.; Cowan, J. A. Biological Coordination Chemistry of Magnesium, Sodium, and Potassium Ions. Protein and Nucleotide Binding Sites. *Coord. Chem. Rev.* **1994**, *135–136*, 165–202.
- (40) Daniele, P. G.; Foti, C.; Gianguzza, A.; Prenesti, E.; Sammartano, S. Weak alkali and alkaline earth metal complexes of low molecular weight ligands in aqueous solution. *Coord. Chem. Rev.* **2008**, *252*, 1093–1107.
- (41) Kellwer, S. W.; Kim, H. N.; Mollouk, T. E. Layer-by-Layer Assembly of Intercalation Compounds and Heterostructures on Surfaces: Toward Molecular "Beaker" Epitaxy. *J. Am. Chem. Soc.* **1994**, *116*, 8817–8818.
- (42) Scatchard, G. The attractions of proteins for small molecules and ions. *Ann. N.Y. Acad. Sci.* **1949**, *51*, 660–672.
- (43) Bergmeyer, H. U.; Gawehn, K.; Grassl, M. *Methods of Enzymatic Analysis*, 2nd ed.; Bergmeyer, H. U. ed.; Academic Press: Inc: New York, 2007; Vol. I; p 457–458.
- (44) Hsiao, H. Uedaira. Thermal Stability of Free and Immobilized Glucose Oxidase Studied by Activity Assay and Calorimetry. *Agric. Biol. Chem.* **1989**, *53*, 833.

- (45) Rothe, J.; Plaschke, M.; Denecke, M. A. Understanding Humic Acid/Zr(IV) Interaction – A Spectromicroscopy Approach. *AIP Conf. Proc.* **2007**, *882*, 193–195.
- (46) Tshuvu, E. Y.; Goldberg, I.; Kol, M. Zirconium Complexes of Amine Bis(phenolate) Ligands as Catalysts for 1-Hexene Polymerization: Peripheral Structural Parameters Strongly Affect Reactivity. *Organometallics* **2001**, *20*, 3017–3028.
- (47) Harding, M. M. The architecture of metal coordination groups in proteins. *Acta Crystallogr.* **2004**, *D60*, 849–859.
- (48) Cao, L. *Carrier-bound Immobilized Enzymes: Principles, Application and Design*; Wiley-VCH: New York, 2006.
- (49) Matoba, S.; Tsuneda, S.; Saito, K.; Sugo, T. Highly Efficient Enzyme Recovery Using a Porous Membrane with Immobilized Tentacle Polymer Chains. *Nat. Biotechnol.* **1995**, *13*, 795–797.
- (50) Cheng, H.; Zhang, K.; Libera, J. A.; de la Cruz, M. O.; Bedzyk, M. J. Polynucleotide Adsorption to Negatively Charged Surfaces in Divalent Salt Solutions. *Biophys. J.* **2006**, *90*, 1164–1174.